electronics

*Article*

# Automated Detection of Alzheimer's via Hybrid Classical Quantum Neural Networks

**Tayyaba Shahwar [1], Junaid Zafar [1,*], Ahmad Almogren [2], Haroon Zafar [3,4,5], Ateeq Ur Rehman [1], Muhammad Shafiq [6,*] and Habib Hamam [7,8,9]**

[1] Department of Electrical Engineering, Government College University, Lahore 54000, Pakistan; tayyabaniazi28@gmail.com (T.S.); ateeq.rehman@gcu.edu.pk (A.U.R.)
[2] Department of Computer Science, College of Computer and Information Sciences, King Saud University, Riyadh 11633, Saudi Arabia; ahalmogren@ksu.edu.sa
[3] Cardiovascular Research & Innovation Centre Ireland, School of Medicine, National University of Ireland Galway, H91 TX33 Galway, Ireland; haroon.zafar@nuigalway.ie
[4] Lambe Institute for Translational Research, National University of Ireland Galway, H91 TX33 Galway, Ireland
[5] College of Engineering and Informatics, National University of Ireland Galway, H91 TX33 Galway, Ireland
[6] Department of Information and Communication Engineering, Yeungnam University, Gyeongsan 38541, Korea
[7] Faculty of Engineering, Uni de Moncton, Moncton, NB E1A3E9, Canada; habib.hamam@umoncton.ca
[8] International Institute of Technology and Management, Libreville BP1989, Gabon
[9] School of Electrical Engineering, Department of Electrical and Electronic Engineering Science, University of Johannesburg, Johannesburg 2006, South Africa
* Correspondence: chairperson.engineering@gcu.edu.pk (J.Z.); shafiq@ynu.ac.kr (M.S.)

**Abstract:** Deep Neural Networks have offered numerous innovative solutions to brain-related diseases including Alzheimer's. However, there are still a few standpoints in terms of diagnosis and planning that can be transformed via quantum Machine Learning (QML). In this study, we present a hybrid classical–quantum machine learning model for the detection of Alzheimer's using 6400 labeled MRI scans with two classes. Hybrid classical–quantum transfer learning is used, which makes it possible to optimally pre-process complex and high-dimensional data. Classical neural networks extract high-dimensional features and embed informative feature vectors into a quantum processor. We use resnet34 to extract features from the image and feed a 512-feature vector to our quantum variational circuit (QVC) to generate a four-feature vector for precise decision boundaries. Adam optimizer is used to exploit the adaptive learning rate corresponding to each parameter based on first- and second-order gradients. Furthermore, to validate the model, different quantum simulators (PennyLane, qiskit.aer and qiskit.basicaer) are used for the detection of the demented and non-demented images. The learning rate is set to $10^{-4}$ for and optimized quantum depth of six layers, resulting in a training accuracy of 99.1% and a classification accuracy of 97.2% for 20 epochs. The hybrid classical–quantum network significantly outperformed the classical network, as the classification accuracy achieved by the classical transfer learning model was 92%. Thus, a hybrid transfer-learning model is used for binary detection, in which a quantum circuit improves the performance of a pre-trained ResNet34 architecture. Therefore, this work offers a method for selecting an optimal approach for detecting Alzheimer's disease. The proposed model not only allows for the automated detection of Alzheimer's but would also speed up the process significantly in clinical settings.

**Keywords:** machine learning; deep neural network; quantum computing; quantum machine learning; quantum neural network; Alzheimer's disease

check for updates

**Citation:** Shahwar, T.; Zafar, J.; Almogren, A.; Zafar, H.; Rehman, A.U.; Shafiq, M.; Hamam, H. Automated Detection of Alzheimer's via Hybrid Classical Quantum Neural Networks. *Electronics* **2022**, *11*, 721. https://doi.org/10.3390/electronics11050721

Academic Editor: Amir Mosavi

Received: 28 January 2022
Accepted: 24 February 2022
Published: 26 February 2022



## 1. Introduction

According to the World Health Organization, Alzheimer's disease will be a serious health burden in coming times, as approximately 24 million people are affected worldwide, and this number is anticipated to double every 20 years [1]. Against this backdrop, Deep

Neural Networks (DNNs) and Quantum Computing (QC) are continuously nurturing healthcare systems and modalities [2–6]. Unprecedented advances in DCCs have already influenced the computer vision area, including medical imaging [7]. Out-of-set generalization had remained a challenge for Computer Vision, which has been resolved with the availability of recurrence and feedforward learning networks. DNNs can be used to find hidden patterns from the data and learn the classification decision boundaries concurrently, thus skipping the tedious step of feature engineering, making them a viable choice for medical imaging modalities [8]. In [9], it was reported that rather than training an entire model from the start, it is better to begin from an already-trained deep neural network and then adjust the last layers for the medical image dataset. Stacked de-noising auto-encoders were used for feature extraction from the multi-modal dataset of the Alzheimer's Neuroimaging Program (ADP). Ref [10–12], ensemble and clustering networks were presented for the detection of Alzheimer's disease from MRI scans. Similarly, different DNNs have been suggested for the classification of Alzheimer's using DemNet, LeNet, and AlexNet with reasonable accuracies [13,14].

However, the suggested algorithms were tested against small datasets. For larger medical imaging datasets, tremendous speed-up potential lies in hybrid classical–quantum machine learning networks. Quantum machine learning (QML) implements quantum circuits based on the variational principle to achieve the desired classification accuracy along with increased speed [15–18]. We focus particularly on hybrid models implementing quantum variational circuits [19–25] and classical neural networks for computationally intensive feature extraction tasks. Similarly, the concept of transfer learning is yet to be validated, as limited reported literature is available in this context [26–29].

To the best of the authors' knowledge, classical–quantum hybrid networks have so far not been used to characterize brain-related diseases using imaging techniques. Therefore, the authors propose a novel hybrid classical–quantum deep neural network to detect Alzheimer's using MRI scans. A large dataset, publicly available in the form of MRI scans of 6400 labeled images with balanced classes, is used to train our network. The labeled images are symmetrically distributed into binary classes, namely, demented and non-demented. ResNet 34 is used to extract features in the classical machine learning domain by using adaptive average pooling before the fully connected stage. After four layers with a mix of convolutional, batch normalization, ReLu, and max pool operations, a 512-feature vector is extracted. Then, data are fed further to a dressed quantum variational circuit without fully connected layer. Embedding of the variational circuit is performed using Hadamard and rotational gates followed by an entanglement stage implemented via CNOT gates, which is further fed to the measurement stage. Hybrid transfer learning is used, which makes it possible to optimally pre-process high-dimensional data and embed them into a quantum processor. The quantum variational circuit gives the output of a four-dimensional vector. According to the binary classification problem, a fully connected layer reduces the four-dimensional vector to a two-dimensional vector. The network learned with variational quantum circuit and ResNet3four-feature vector to classify demented and non-demented MRI images.

The key contributions of this study are as follows:

- A novel classical–quantum model using modified ResNet34 architecture and a variational circuit were designed with selected learning parameters for both domains. MRI images are similar between clinical settings; therefore, this model is useful for accurate model training/testing.
- Secondly, a reasonable dataset size was trained and tested that is suggestive that the potential of quantum computing in the middle layer of deep neural networks was unlocked for dimensionality reduction.
- The third main contribution of this research is the implementation of transfer learning for classical–quantum hybrid networks consisting of MRI images, and their validation through different quantum packages including PennyLane default simulator, qiskit.aer, and qiskit.basicaer.

The paper is structured as follows: The Materials and Methods are presented in Section 2, in which the classical model, variational quantum circuit, and hybrid model are explained. Further transfer learning methods, dataset description, and data pre-processing are also presented. The experimental results using the classical model and the quantum model are explained in Section 3. The discussion and conclusion of the paper are presented in Sections 4 and 5, respectively.

## 2. Materials and Methods

### 2.1. Classical Neural Networks

A classical deep neural network permits raw data to be received as the input to the network, automatically discovering all necessary relationships for performing classification. It is possible to build a hierarchical structure of different nodes that can learn and calculate nonlinear mapping on their own, called deep neural networks (DNNs). A deep learning network involves a sequence of hierarchically structured nodes. The complete classical network is the concatenation of many layers. The equation for the feed-forward neural network is given as [30]:

$$Li = \sum_{i=1}^{n} x_i \rightarrow y_i = \phi(Wx_i + b) \tag{1}$$

where $Li$ is called the layer of the network, $x_i$ is the input vector and $y_i$ is the output vector, $W$ is weights and $b$ is biases, and $\phi$ is a nonlinear activation function.

ResNet34 is a convolutional neural network architecture that consists of 34 layers, and it has been used as a classical transfer learning model for Alzheimer's disease detection. A schematic representation of ResNet34 architecture is shown in Figure 1. It consists of convolution, batch normalization, ReLU, and max pooling operations trailed by four layers: layer 1, layer 2, layer 3, and layer 4. At the end of architecture, ResNet34 includes an adaptive average pooling layer and a fully connected layer that has a 1000-output feature vector.

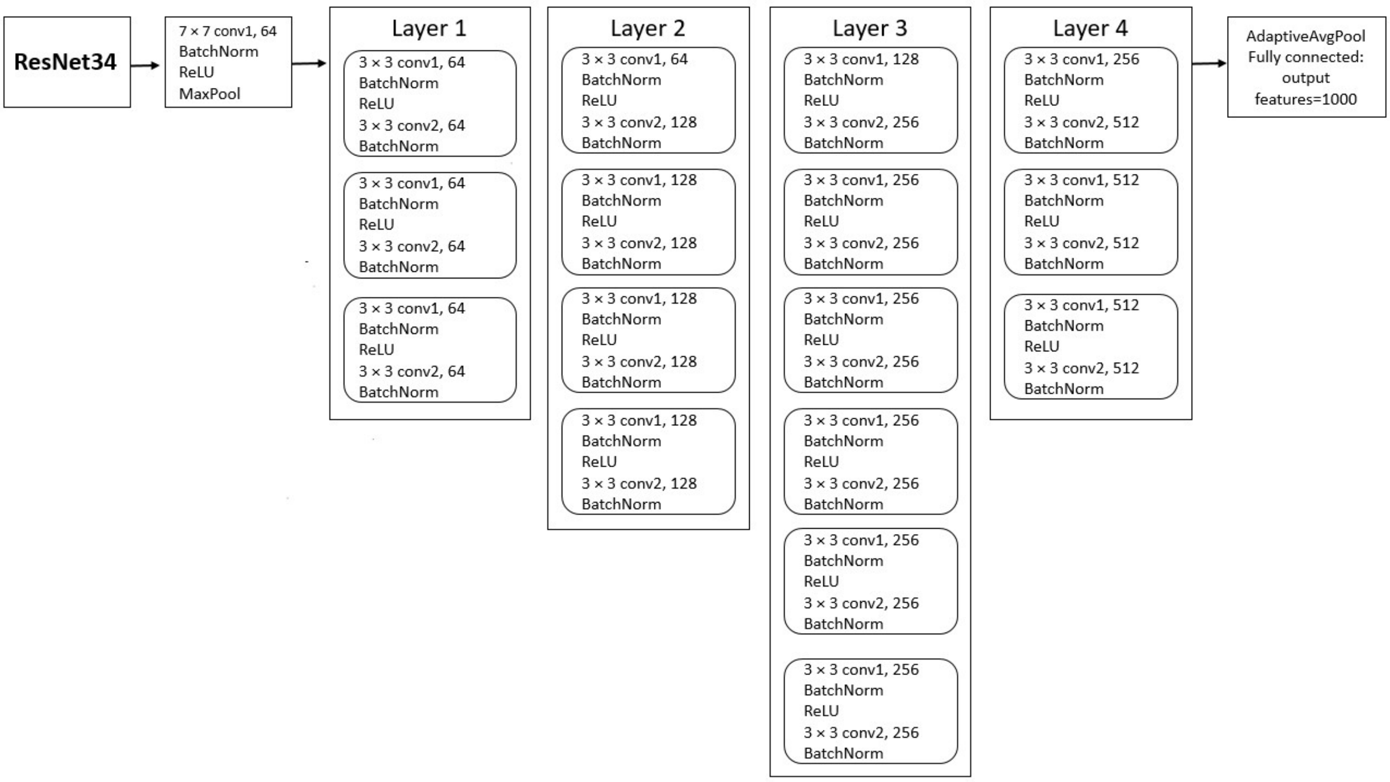


**Figure 1.** A schematic representation of Resnet34 architecture.

### 2.2. Quantum Variational Circuit

Before explaining the quantum variational circuit, it is important to describe some of the fundamentals of quantum computing.

In quantum computers, the quantum bit is the basic component of quantum info, which signifies subatomic elements such as the memory of a computer. It can take values of 0, 1, or both. It is a billion times more powerful than the most powerful laptops [31]. A qubit has two quantum states. Quantum bits can be 1, 0, or in both states at the same time. These quantum states are represented in the form of notation, known as Dirac representation. Hence, states are transcribed as $|0\rangle$ and $|1\rangle$. Therefore, qubits are represented as two-state linear combinations, each with its complex coefficient, i.e., $|w\rangle = x\,|0\rangle + y\,|1\rangle$, where x and y are the coefficients of the two states. When a quantum bit is measured, the outcome produces a $|0\rangle$ state with a probability equivalent to $|x|^2$ or a $|1\rangle$ state with a probability equivalent to $|y|^2$ [31].

Superposition is an underlying principle of quantum mechanics. Superposition names the capacity of those systems in which qubits can occur in multiple states simultaneously. This renders high-speed parallel processing possible, and is significantly different from its classical equivalents. In classical computers, if we have 2 bits, there are 4 possible outcomes, which can be only 1 value at any given instant. However, on the other hand, if there are two quantum bits in a quantum computer, the total number of combined possible values is 4, and all values exist at the same time [31].

Entanglement is a fundamental property of quantum computing, and denotes a resilient connection between two quantum bits. If the quantum bits are separated by a large distance, they are connected through impeccable connections. These quantum bits are entangled with each other, whereby the behavior of one bit affects the behavior of the other. This generates powerful communication among quantum bits. Once they have been entangled, they will remain connected, even at opposite ends of the universe. In a classical computer, if the number of digits doubles, so does the computing power. However, in entanglement phenomena, the accumulation of more data in a quantum computer can cause its computing power to exponentially surge [31].

In quantum computing, quantum gates are used to manipulate quantum bits and their quantum state. Quantum gates, including single-qubit gates, such as the Hadamard gate, and multiple-qubit gates, such as the CNOT gate, are used to operate quantum bits. A quantum circuit is a sequence of quantum gates applied to a register of n quantum bits.

Quantum computing uses quantum circuits that consist of qubits and quantum gates. A quantum bit is the basic element of quantum information, and is analogous to classical bits. Similarly, quantum gates are analogous to classical gates, and act as the major blocks in quantum variational circuits. However, quantum gates differ from classical logic gates in that they execute mathematical operations on several qubits, representing a unitary transformation. A variational quantum circuit consists of quantum gates with a fixed depth. This is the central part of the quantum layer for executing mathematical operations. A quantum circuit consists of single-qubit gates as well as multiple-qubit gates.

A quantum variational circuit consists of a state preparation layer (the initialization state followed by Hadamard gates), variational layers (a series of rotational gates followed by Controlled Not gates), and a measurement layer (mapping of quantum vector space onto the classical vector space), as shown in Figure 2.

Variational quantum circuits consist of four parts.

**Initialization:** All 4 qubits initialize in the $|0\rangle$ state. Then, quantum bits are given as an input to the quantum gate called the Hadamard gate, in order to carry all quantum bits into a superposition state.

**Embedding layer:** This layer converts the standard input in a quantum circuit by embedding a classical vector into a quantum vector by using Hadamard gates and rotational gates.

**Variational layers:** A sequence of trainable rotation layers and constant entanglement layers are applied. Entanglement layers can be created using Controlled Not gates.

**Measurement layer:** For 4 qubits, the expectation value is measured. This produces a classical output vector.

The entire quantum variational circuit, including the embedding layer, variational layer, and final measurement layer, can be expressed as:

$$Q = |x\rangle \to y = \{\langle x|\hat{y}|x\rangle \cdot (\ L_d \ldots L_1) \cdot Ex/0\}. \quad (2)$$

$\langle x|\hat{y}|x\rangle$ is the measurement layer, and consists of a mapping from the quantum vector to a classical vector, $L$ is the layer of the quantum circuit, and $d$ is the depth of the variational circuit. $E$ is an embedding layer that depends on $x$ and ground truth. The embedding layer is a mapping from the classical vector to the Hilbert space vector.

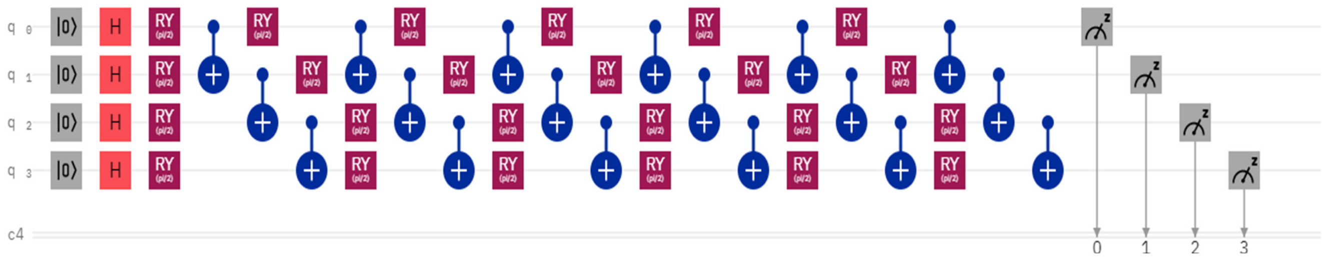

**Figure 2.** Quantum variational circuit. H symbol denote Hadamard gate, RY symbol denote rotational Y gate, + symbol denote CNOT gate. z symbol denotes measurement stage.

Quantum algorithms are generally defined by a quantum circuit that applies to quantum bits and ends by measuring the quantum bits. Quantum circuits consist of quantum gates, such as the Hadamard gate and CNOT gate, that act on a quantum bit. The operation of a quantum algorithm normally starts by initializing the states, entangling the states, and measuring the states as demonstrated in Algorithm 1. The first step in the quantum algorithm is to prepare the test kernel using the dataset. The dataset is described as $D = \{(x_i,\ y_i)\}$. Then, quantum circuits convert classical data into quantum bits to execute complex computations in high-dimensional Hilbert space. In order to manipulate the quantum states into superposition states and entangling states, quantum gates are used, and this can be performed by taking the inner product over superposition states. Lastly, we measure the quantum states, which provides a classical outcome using the distribution function, and we update the parameter using classical post-processing.

The algorithm for the quantum variational circuit is given below, in which $D$ is the dataset containing the input vector $x_i$ and output vector $y_i$, n is the number of elements, $K$ is the kernel function, and F(D) is the distribution function.

**Algorithm 1.** Quantum Variational Circuit.

Data Input (D)

$D = \{(x_i,\ y_i)\}.$ // Prepare test kernel into QRAM using Dataset (D)

$\frac{1}{\sqrt{n}} \sum_{i=1}^{n} |i\rangle|x \cdot x_i\rangle$ // Amplitude Q median estimation

$\frac{1}{\sqrt{n}} \sum_{i=1}^{n} |i\rangle|K(x_* \quad \cdot x_i)\rangle$ // Inner product over superposition

$|K_*\rangle = \frac{1}{\sqrt{F(D)}} \sum_{i=1}^{n} K(x_* \cdot x_i)|i\rangle.$ // Measurement to prepare using tangent kernel

Output $|K_*$

## 2.3. Hybrid Classical–Quantum Neural Network

The quantum neural network model is an amalgamation of classical and quantum neural networks. Figure 3 shows a representation of data processing using a classical–quantum neural network. It consists of a feature vector of the classical network, a variational quantum circuit, and a fully connected layer of the classical network that classifies Alzheimer's disease using demented and non-demented MRI images. In this work, a convolution neural network architecture called ResNet34 was used as a feature extractor. This was used to simplify the given input image into a 512-feature vector. Then, dimensionality reduction was performed using the quantum variational circuit.

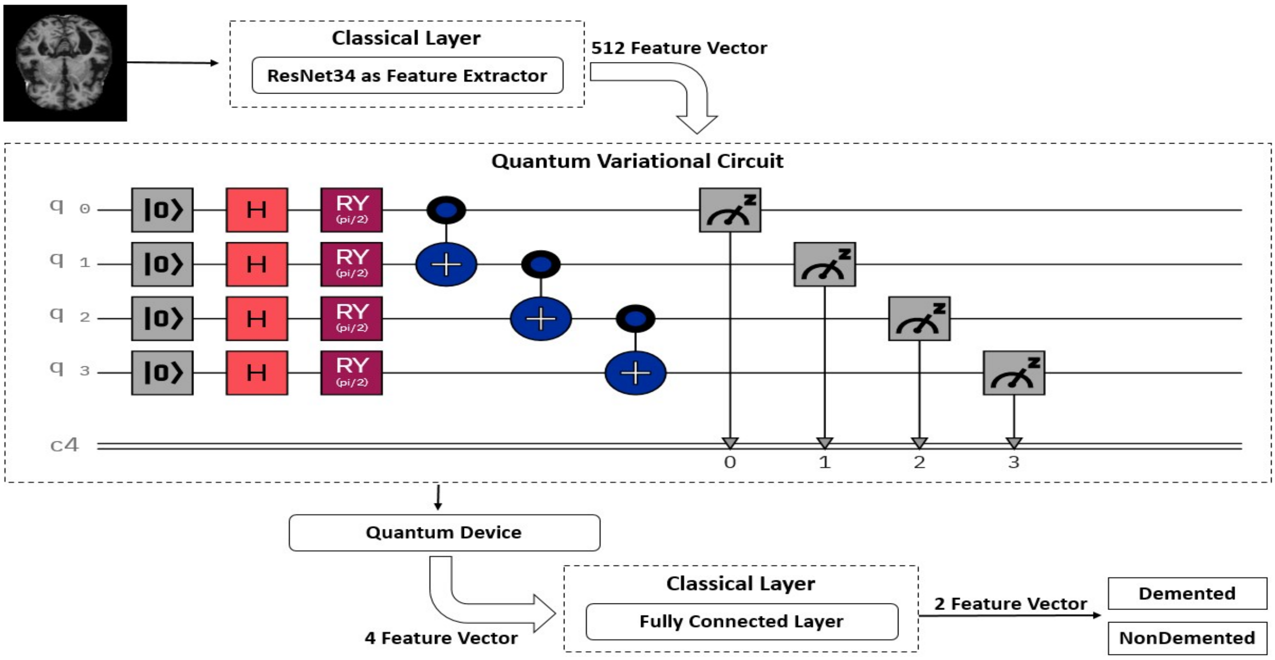


**Figure 3.** Demonstration of data processing using quantum–classical transfer learning.

The 512-feature vector given by the residual neural network was converted to 4 dimensions by using a variational quantum circuit. The quantum circuit gives a four-dimensional vector as output. Then, a fully connected layer was used to reduce the four-dimensional vector to a two-dimensional vector. The network learned by means of the variational quantum circuit and the ResNet3 four-feature vector to classify demented and non-demented MRI images. The hybrid quantum neural network, consisting of 512 input features and 2 output features, can be written as follows [30]:

$$\mathrm{L}_{4\rightarrow 2} \cdot \mathrm{Q} \cdot \mathrm{L}_{512\rightarrow 4} \tag{3}$$

where $\mathrm{L}_{512\rightarrow 4}$ denotes a classical layer, Q is a quantum variational circuit, and $\mathrm{L}_{4\rightarrow 2}$ is a binary classification layer.

### *2.4. Transfer Learning*

It has been reported that in many cases, rather than training an entire model from the beginning, it is better to start with an already-trained deep neural network and then adjust the last layer to perform specific tasks. Transfer learning is basically a technique used for solving small numbers of dataset problems using deep neural networks. If a previously trained deep neural network can successfully solve specific problems, the network can be reused to decipher different but similar problems. In deep learning, transfer learning methods include:

1. Fine-tuning: here, pre-trained models are loaded and used for training. This eliminates the burden of random initialization on the neural network.
2. Feature extraction: like fine-tuning, the pre-trained model is loaded, and then the weight of all layers is frozen, except for the last layer, which is then used for training.

This architecture may be optimized depending upon the requirements of the dataset. The variational formula is normally decomposed into two stages: classical-to-classical transfer learning and classical-to-quantum transfer learning, as shown in Figure 4.

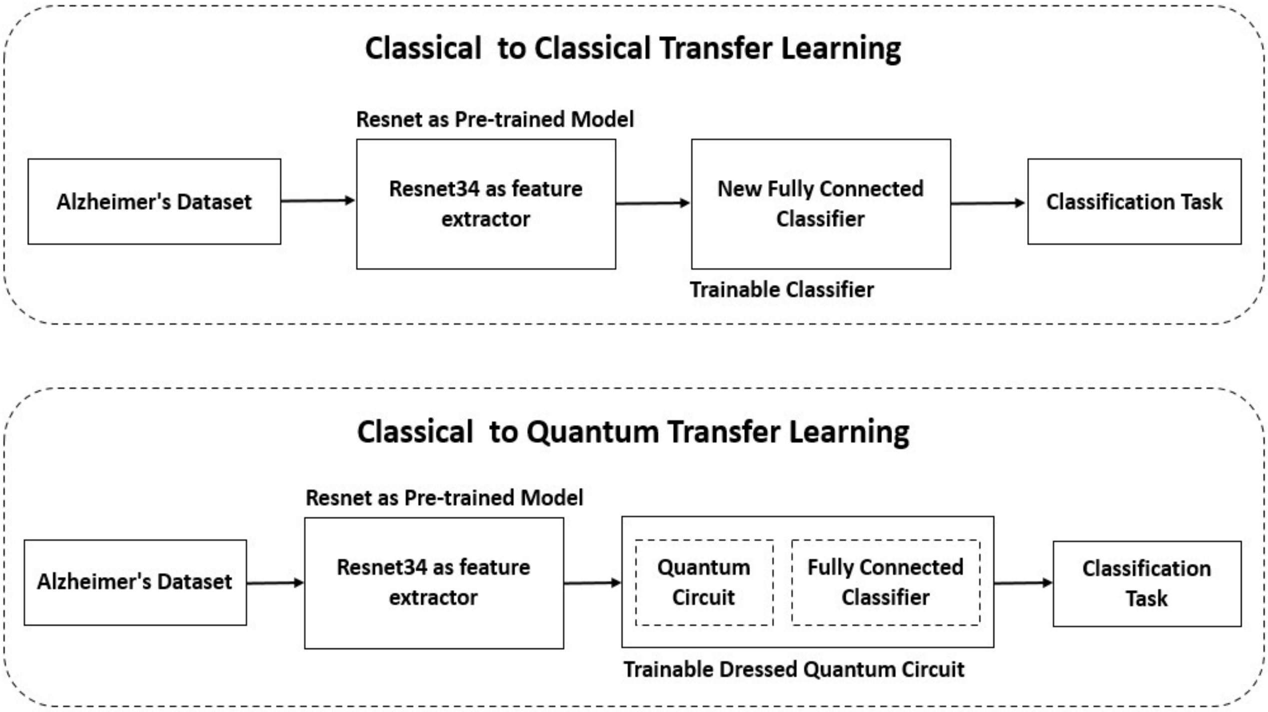


**Figure 4.** Illustration of hybrid classical to quantum transfer learning.

The first is classical-to-classical transfer learning, in which ResNet34 is used as a pre-trained model by preserving all convolutional and pooling layers, and a new trainable classifier is added to the network to classify the MRI images.

The second is classical-to-quantum transfer learning, in which a classical pre-trained model such as ResNet34 is used as a feature extractor, and a trainable dressed quantum circuit is added to the network to classify MRI images. This hybrid method is suitable for handling high-resolution images, because significant features are applied to the quantum variational circuit. We employed a classical-to-quantum transfer learning method for the binary detection of Alzheimer's disease using different simulators, as presented in Section 3.

*2.5. Dataset Description*

In this work, the dataset was taken from the Kaggle platform. They provide the relevant data containing demented and non-demented MRI scans. A labeled dataset consisting of 6400 MRI scans was used for the classification of Alzheimer's disease [32]. The size of the images in the dataset is 176 × 208.

First, a balanced dataset was used to train and test a deep transfer learning model and quantum transfer learning model, because it contains an equal number of samples from the demented and non-demented classes. The Alzheimer's dataset was divided into two categories, marked as demented and non-demented. The dataset was distributed as follows: 90% was apportioned to the training dataset and 10% to the testing dataset. The training dataset was used to train the network, and the testing dataset was used for prediction.

Second, the unbalanced dataset was also used to train and test a quantum transfer learning model. The dataset was distributed as follows: 90% was apportioned to the training dataset and 10% to the testing dataset. The training dataset was used to train the network, and the testing dataset was used for prediction.

### 2.6. Data Pre-Processing

The pre-processing stage consists of three steps. First, MRI images were center cropped to 224 × 224 pixels, then converted to PyTorch tensor, and lastly, image normalization was performed based on the mean and standard deviation.

## 3. Results and Analysis

### 3.1. Experiment #1

#### 3.1.1. Alzheimer's Detection Using Transfer Learning

In this experiment, MRI classification tasks using deep neural network architecture were implemented. Transfer learning using pre-trained models such as GoogleNet and ResNet34 were implemented, and inter comparative performance analysis was performed.

#### 3.1.2. Hyperparameters in Deep Learning

Hyperparameters are variables that are required to be set first, before applying the learning algorithm of the dataset.

Learning rate is one of the hyperparameters in the optimizer. The learning rate controls the step to achieve a minimal loss function. If the learning rate is higher, the model learns faster, but it may not achieve minimal loss function. If the learning rate is lower, there will be a better chance of achieving the minimum loss function, but more epochs and computational resources will be required.

Batch size is a hyperparameter used in deep learning. The batch size denotes the number of training samples used as an input. Smaller batch sizes make the learning process faster, whereas larger batch sizes result in a slower learning process.

Epochs are defined as the number of times an entire data set passes through a deep neural network model. One epoch indicates that the complete training dataset is passed forward and backward throughout the model. Smaller numbers of epochs lead to underfitting, while too many epochs result in overfitting. The epoch number must be adjusted in order to achieve the best results.

The loss function computes the performance of the neural network when carrying out specific regression or classification tasks. During backpropagation, the loss function should be minimized in order to improve the neural network. The cross-entropy loss function is used for classification. The mean squared error loss function is used for regression. The cross-entropy loss function for binary classification is given as [33]:

$$CEL = -\sum_{n=1}^{2} y_n \log(P_n). \tag{4}$$

where $y_n$. is the output value and $P_n$ is the probability of the $n$th class.

The Adam (Adaptive Moment Estimation) optimizer is an optimization algorithm used to train the neural network. It is computationally powerful and ideal for bigger datasets. It does not require much memory. This method is very effective for dealing with large problems involving large amounts of data or numbers of parameters. The hyperparameters of the GoogleNet model and the ResNet34 model are given in Table 1.

**Table 1.** Hyperparameters of the GoogleNet and Resnet34 model.

| Hyperparameters | Learning Rate | Optimization Algorithm | Loss Function | Epochs | Batch Size | Weight Decay |
|---|---|---|---|---|---|---|
| Value/Name | $10^{-4}$ | Adam Optimizer | Cross Entropy | 20 | 16 | $1 \times 10^{-4}$ |

#### 3.1.3. GoogleNet Model

The GoogleNet architecture has been used for classifying MRI images. The GoogleNet architecture uses an RGB color channel with images with a size of 224 × 224. The overall architecture has 22 layers. GoogleNet practices 1 × 1 convolution in its network. Convolutional layers are used to reduce the number of parameters. The GoogleNet architecture uses a technique called "global average pooling". This lessens the number of trainable parameters and progresses the accuracy.

#### 3.1.4. ResNet Model

The ResNet model is the most prevalent and effective deep learning model. The residual units are made up of convolutional layers and pooling layers. In this network, a technique called skipping connections was used. Skipping connections skips several layers of training and attaches directly to the output. ResNet34 performed better than GoogleNet in terms of accuracy, precision, recall, and F1-score. Therefore, in this work, the Resnet34 architecture was preferred in terms of training accuracy and training loss with respect to iteration. The training accuracy of ResNet34 was higher than that of GoogleNet. Training accuracy and training loss with respect to epochs are illustrated in Figures 5 and 6.

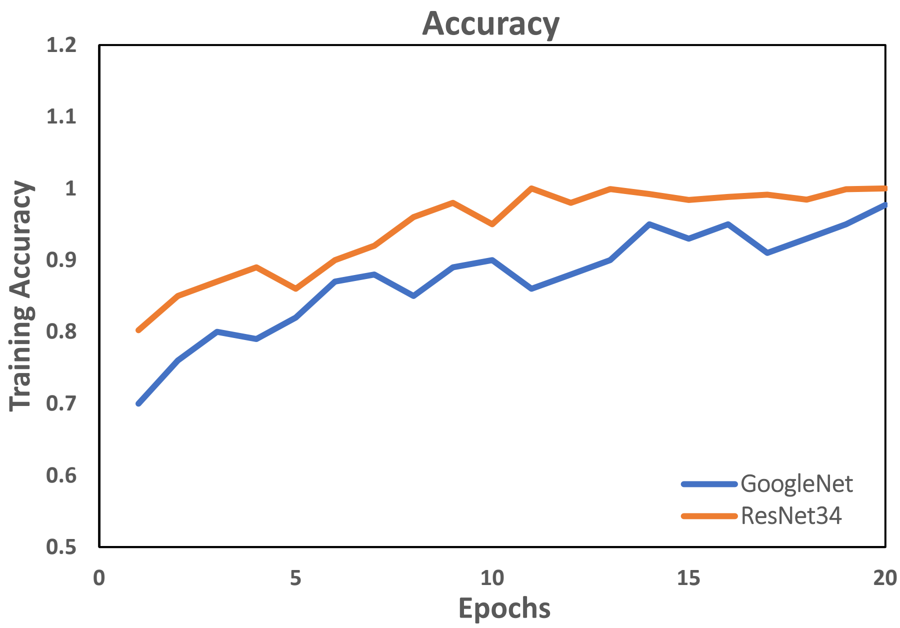


**Figure 5.** Training accuracy with respect to epochs.

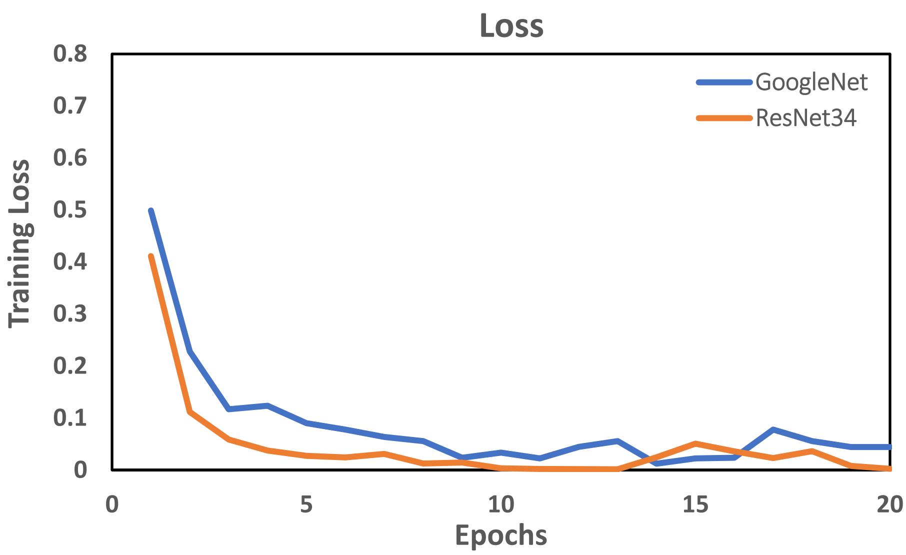


**Figure 6.** Training loss with respect to epochs.

Performance metrics such as accuracy, recall, precision, and F1-score were measured to evaluate the model, and these are given as follows [34]:

$$\text{Acc} = \frac{\text{TP} + \text{TN}}{\text{TP} + \text{TN} + \text{FP} + \text{FN}} \tag{5}$$

$$\text{Recall} = \frac{\text{TP}}{\text{TP} + \text{FN}} \tag{6}$$

$$\text{Precision} = \frac{\text{TP}}{\text{TP} + \text{FP}} \tag{7}$$

$$\text{F1} - \text{score} = 2 \times \frac{\text{Recall} \times \text{Precision}}{\text{Recall} + \text{Precision}} \tag{8}$$

TP is True Positive, and describes correctly predicted positive examples. FP is False Positive, and describes as falsely predicted positive examples. TN is True Negative, and describes correctly predicted negative examples. FN is False Negative, and describes falsely predicted negative examples. The results of the GoogleNet model and the ResNet34 model are given in Table 2. The confusion matrix for GoogleNet and ResNet34 are presented in Figure 7.

**Table 2.** Results of the GoogleNet and ResNet34 models.

| Model | Training Accuracy | Validation Accuracy | Testing Accuracy | Recall | Precision | F1-Score |
|---|---|---|---|---|---|---|
| GoogleNet | 0.97 | 0.97 | 0.89 | 0.92 | 0.89 | 0.87 |
| Resnet34 | 1.00 | 0.98 | 0.92 | 0.94 | 0.92 | 0.92 |

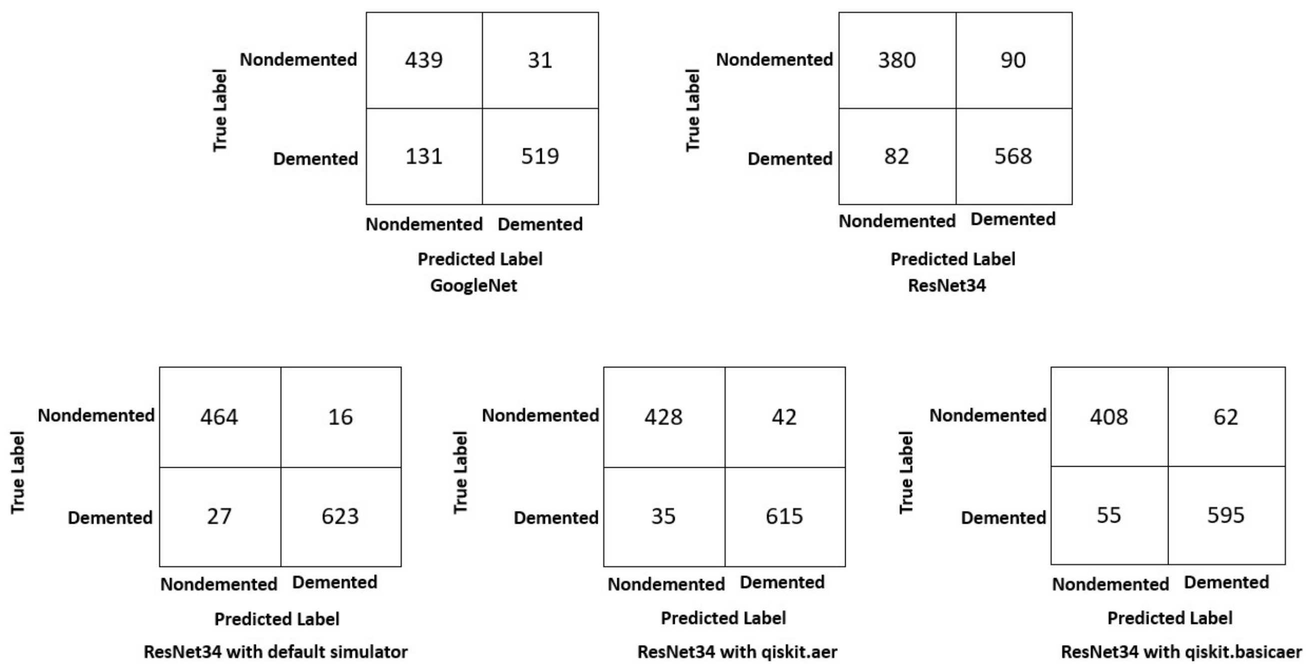


**Figure 7.** Confusion matrix for the demented and non-demented labels using GoogleNet, ResNet34 and different quantum simulators.

### 3.2. *Experiment #2*

#### 3.2.1. Alzheimer's Detection Using Quantum Transfer Learning

In this experiment, MRI classification and prediction tasks were implemented using deep neural network architecture through the quantum transfer learning model. This is a hybrid classical–quantum neural network containing a feature vector of ResNet34 and a variational network. The classical network is a ResNet34 Network, with its inputs, weights, and biases. The quantum circuit is a variational quantum circuit with qubits, rotations, and CNOT gates. In hybrid models, quantum variational circuits and pre-trained classical convolutional neural networks are mutually trained to detect the presence of Alzheimer's disease. The network learns to classify demented and non-demented MRI images by means of the variational quantum circuit and the resNet3four-feature vector. Different quantum simulators, such as the PennyLane default simulator, the qiskit.aer simulator, and the qiskit.basicaer simulator, as well as the PyTorch deep learning framework, were used to perform Alzheimer's disease detection using the quantum transfer learning method. The hyperparameters of the classical–quantum neural network is given in Table 3.

**Table 3.** Hyperparameters of the classical–quantum neural network.

| Hyperparameters | Learning Rate | Loss Function | Optimization Algorithm | Epochs | Batch Size | Weight Decay | Quantum Depth | Quantum Delta |
|---|---|---|---|---|---|---|---|---|
| Value/Name | $10^{-4}$ | Cross Entropy | Adam Optimizer | 20 | 8 | $1 \times 10^{-4}$ | 6 | 0.01 |

### 3.2.2. Quantum Transfer Learning Using PennyLane

PennyLane library [35] was used for the implementation of the hybrid quantum–classical neural network. The PennyLane 'default.qubit' simulator [35] was used for the implementation of the hybrid quantum–classical neural network. ResNet34 was used as a classical neural network and a variational quantum circuit was added to the network for the classification of MRI images. The training accuracy and validation accuracy plots, as well as the training loss and validation loss plots, are shown in Figure 8 for the PennyLane default simulator with ResNet34.

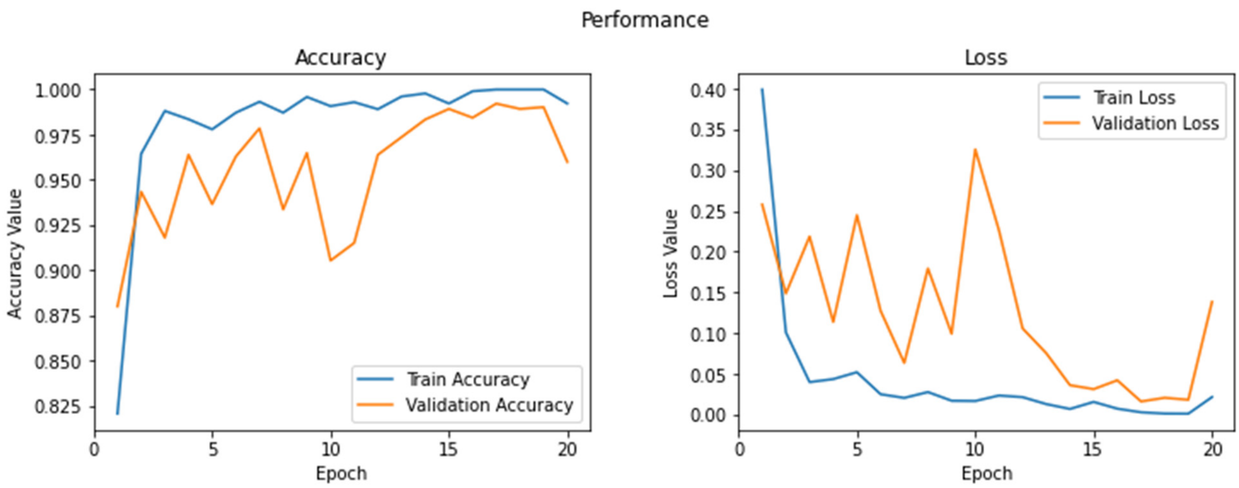


**Figure 8.** Accuracy plot and loss plot for pennyLane default simulator with ResNet34.

### 3.2.3. Quantum Transfer Learning Using the PennyLane-Qiskit Plugin

The PennyLane-Qiskit plugin combines the Qiskit quantum computing framework and PennyLane's quantum machine learning. By installing the PennyLane-Qiskit plugin, Qiskit devices can be obtained in PennyLane. At the present time, three devices are available, named 'qiskit.aer', 'qiskit.basicaer', and 'qiskit.ibmq' [35]. In this work, 'qiskit.basicaer' and 'qiskit.aer' were used for the implementation of quantum transfer learning. The accuracy plot and the loss plot for qiskit.aer with ResNet34 and for qiskit.basicaer with ResNet34 are shown in Figures 9 and 10.

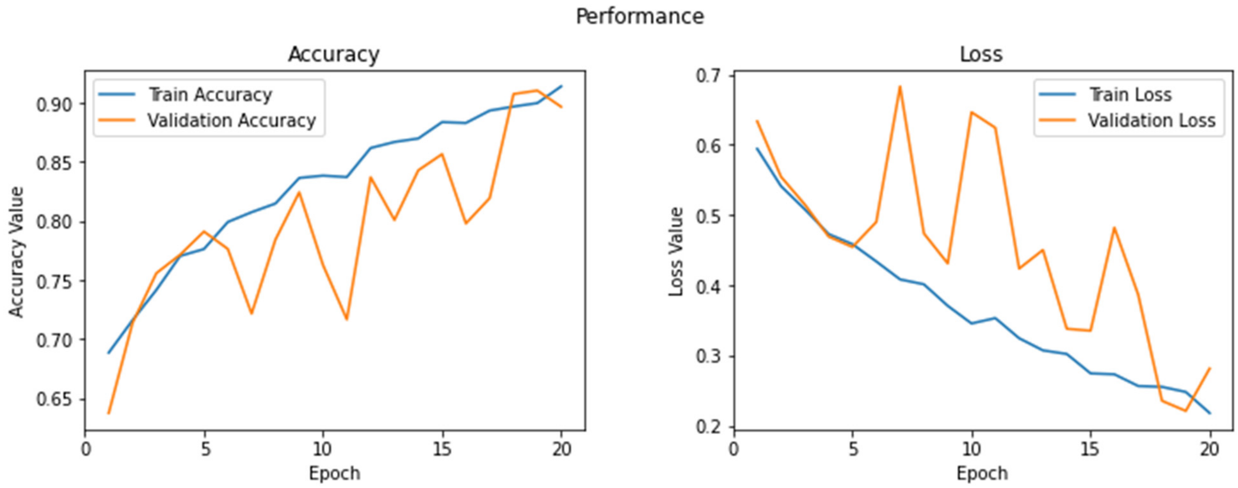


**Figure 9.** Accuracy plot and loss plot for qiskit.aer with ResNet34.

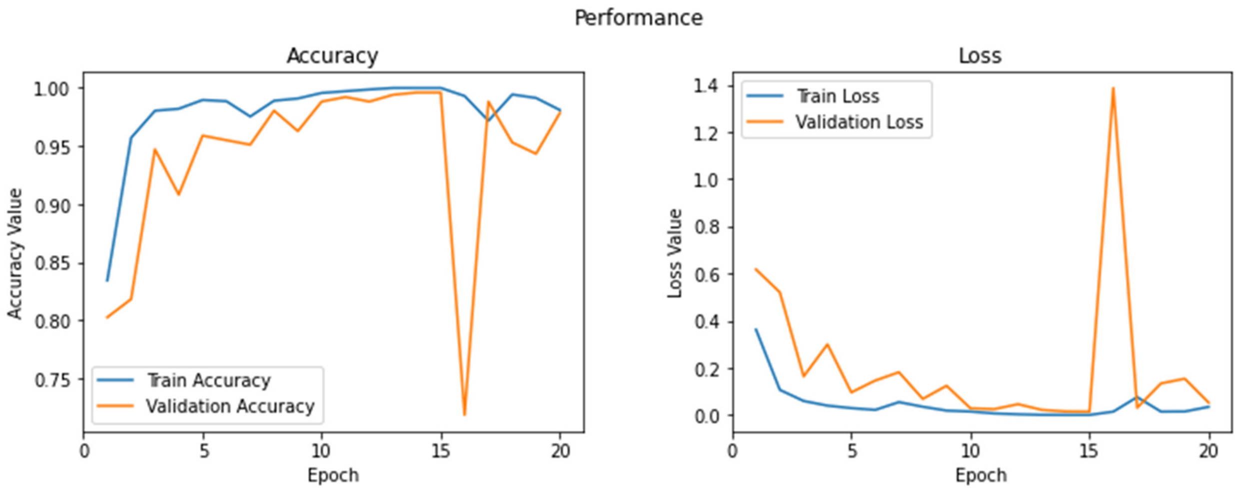


**Figure 10.** Accuracy plot and loss plot for qiskit.basicaer with ResNet34.

The results of the quantum transfer learning model using the PennyLane default simulator, qiskit.aer, and qiskit.basicaer are given in Table 4. The confusion matrix is presented in Figure 7.

**Table 4.** Results of quantum transfer learning model using the balanced dataset.

| Model and Device | Training Accuracy | Validation Accuracy | Testing Accuracy | Precision | F1-Score | Recall |
|---|---|---|---|---|---|---|
| PennyLane default simulator with resnet34 | 0.99 | 0.98 | 0.97 | 0.88 | 0.86 | 0.85 |
| qiskit.aer with resnet34 | 0.95 | 0.89 | 0.94 | 0.86 | 0.86 | 0.87 |
| qiskit.basicaer with resnet34 | 0.98 | 0.97 | 0.95 | 0.91 | 0.87 | 0.94 |

We trained the quantum transfer learning model using an unbalanced dataset. The hyperparameter values are given in Table 3. The training accuracy and validation accuracy plots, as well as the training loss and validation loss plots, are shown in Figure 11 for the PennyLane default simulator for the quantum transfer learning model with ResNet34. The results of the quantum transfer learning model for an unbalanced dataset are given in Table 5.

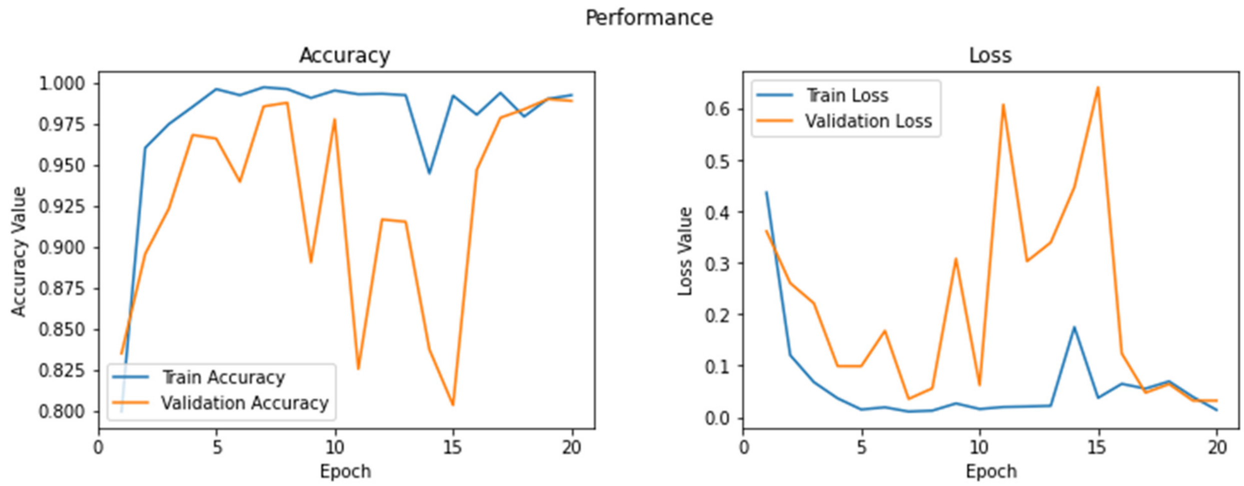


**Figure 11.** Accuracy plot and loss plot for the PennyLane default simulator with ResNet34.

**Table 5.** Results of quantum transfer learning model using an unbalanced dataset.

| Model and Device | Training Accuracy | Validation Accuracy | Testing Accuracy | Precision | F1-Score | Recall |
|---|---|---|---|---|---|---|
| Quantum transfer learning using unbalanced dataset | 0.99 | 0.98 | 0.93 | 0.90 | 0.87 | 0.88 |

In this article, we measured the performance of the classical transfer learning method and the quantum transfer learning method by means of the change in training and validation accuracy and training and validation loss over epochs and architecture. With respect to the overall performance, the training and validation accuracy started at a lower value and gradually increased with increasing number of epochs. As the model underwent more and more iterations, the accuracy increased, while the loss gradually decreased. This process continued until the accuracy and loss reached a constant level. Finally, the quantum simulators and devices were used to train the quantum transfer learning model. The default PennyLane quantum simulator is without noise, and it improved the performance of the model while also increasing the number of trainable parameters in the quantum variational circuit, ultimately providing better results.

The outcomes indicate that transfer learning using a hybrid classical–quantum neural network resulted in improved accuracy, because it learned from an unknown unitary transformation and exhibited resilient sturdiness for the noisy dataset. The quantum transfer learning method has two main benefits when compared with classical transfer learning: resilient expressive and computational power in high-dimensional space due to principles of quantum mechanics such as superposition and entanglement, eventually improving the performance of the model.

## 4. Discussion

Quantum computing offers increased speed, because it is exponentially faster than conventional computers at particular tasks, and it reduces the calculation time from years to seconds. Healthcare data composed using altered modalities such as MRI, PET, CT scans are currently underused. Hence, obtaining meaningful patterns from other areas is perilous. These days, the features of health datasets are diverse and unequally disseminated, resulting in complex computational situation for state-of-the-art models. Therefore, scholars have been investigating ways in which computationally demanding algorithms with healthcare data sources can be sped up using quantum computing methods.

Quantum deep learning is a new research area that endeavors to use quantum computing methods to develop new algorithms and improve conventional machine learning algorithms. Hybrid classical–quantum deep learning based on the ResNet34 architecture harnesses the ability of quantum variational circuits to detect Alzheimer's on the basis of MRI scans. In this model, a convolutional neural network architecture was used to obtain a high-dimensional feature vector. This feature vector was fed to quantum variational circuits consisting of a state preparation layer that was used to encode classical data into quantum data. This layer puts all the qubits into a superposition state through the use of the Hadamard gate, whereby the possible states of the feature vector are estimated. Then, all qubits are entangled with one another by applying three CNOT gates. By using quantum entanglement phenomena, all possible states of the feature vector interacted with each other instantaneously. Therefore, hidden and different patterns were easily discovered. Lastly, a measurement layer was used in order to translate the quantum data into classical data. Therefore, the quantum variational circuit was used to recognize and create a feature vector in a high-dimensional complex Hilbert space, and then the output from the variational quantum circuit was fed to the classifier to detect the MRI images. This quantum transfer learning method has predominantly been significant in the recent period of NISQ technology, because it makes it possible to pre-process high-dimensional input vectors such as images using classical state-of-the-art neural networks, and then to manipulate the highly significant feature vector using a quantum variational circuit.

Quantum computing is the only technology recognized as being exponentially faster than classical computing for particular tasks, and it can help to reduce the calculation time from years to seconds. Quantum computing facilitates the healthcare industry by speeding up diagnosis and medicine customization, and optimizing prices. As the number of approaches to data sources related to health care continues to increase, the amalgamation of quantum computing and classical machine learning for the benefit of society, solving real-time health problems and reducing costs, is increasingly being employed.

Clinical data, such as facts and figures from clinical records, image modality datasets, electronic health records, and medical devices, is increasing. Health-related datasets are variable in nature and unevenly dispersed, creating complex computational tasks for machine learning models. To obtain powerful insights from large and complex datasets, it is necessary to develop substantial models. Regardless of this, classical computing systems are reaching their limits, and this is where the power of quantum algorithms can be leveraged in machine learning applications to improve and speed up the computational algorithms and provide viable solutions for real-time clinical settings.

Quantum circuits integrated with deep learning frameworks can help improve model performance, while also performing computation much more quickly and efficiently when dealing with large datasets. By using a large dataset consisting of 6400 labeled MRI images, it is possible to see an increment in the performance metric compared to classical convolutional neural networks, as hybrid classical–quantum models can more efficiently find complex patterns in datasets.

In the first experiment, a classical convolutional neural network was implemented. GoogleNet and ResNet34, using transfer learning, were used to classify Alzheimer's disease. When applied to an Alzheimer's disease dataset containing MRI images, GoogleNet and ResNet34 showed better results than VGGNet and DenseNet. The testing accuracies achieved using these networks are shown in Table 6.

**Table 6.** Comparison between classical model and quantum transfer learning model.

| Model | Test Accuracy |
|---|---|
| Classical model GoogleNet | 0.89 |
| Classical model ResNet34 | 0.92 |
| Quantum transfer learning model with PennyLane default simulator | 0.97 |
| Quantum transfer learning model with qiskit.basicaer | 0.94 |
| Quantum transfer learning model with qiskit.aer | 0.95 |
| Quantum transfer learning model using unbalanced dataset | 0.93 |

In the second experiment, a quantum–classical neural network was implemented in which ResNet34 was used as a feature extractor, giving 512 dimensions. Then, dimensionality reduction was performed using a quantum variational circuit. Thereby, 512 dimensions were reduced to four dimensions, and then the fully connected layer reduced the four dimensions to two dimensions. The testing accuracies achieved using the quantum transfer learning method with different devices and simulators are shown in Table 6. The testing accuracy achieved using the PennyLane default simulator was higher than that achieved by the other simulators.

These results demonstrate that quantum transfer learning performed better than the classical transfer learning method. The testing accuracy of the quantum model depends on hyperparameters named quantum depth and batch size. Other hyperparameters included the Adam optimizer, used as an optimization algorithm, the cross-entropy function, used as a loss function, and the learning rate, which was set to $10^{-4}$. By using a quantum circuit with a depth of six layers and a batch size set to 8, we trained the quantum transfer learning model and achieved a training accuracy of 99%. This model generalized well on test datasets containing MRI images, achieving an accuracy of 97% when using a balanced dataset. We also trained the quantum transfer learning model using an unbalanced dataset, and achieved a training accuracy of 99%, with this model also generalizing well on the test dataset, achieving an accuracy of 93%. Optimal accuracy was achieved when quantum depth was around 6.

Figure 12 shows a graph of test loss with respect to batch size for the hybrid classical–quantum neural network. Figure 13 shows a graph for test accuracy and quantum depth for the hybrid classical–quantum neural network. The testing accuracy achieved using quantum transfer learning was 0.97 for the default simulator, and 0.94 and 0.95 for the other quantum devices, as shown in Table 6.

On the basis of the analysis of this work, it can be concluded that the hybrid classical–quantum transfer learning method, particularly the classical–quantum implementation in the form of a dressed quantum circuit, improved classification accuracy. Therefore, these experimental result shows that the hybrid classical–quantum neural network performed better than the classical neural network in terms of accuracy, and provided better results.

A comparison of the proposed methodology based on a hybrid classical–quantum neural network with existing methods is presented in Table 7. In addition, this shows that the hybrid classical–quantum deep learning model stands out as being better than the state-of-the-art models.

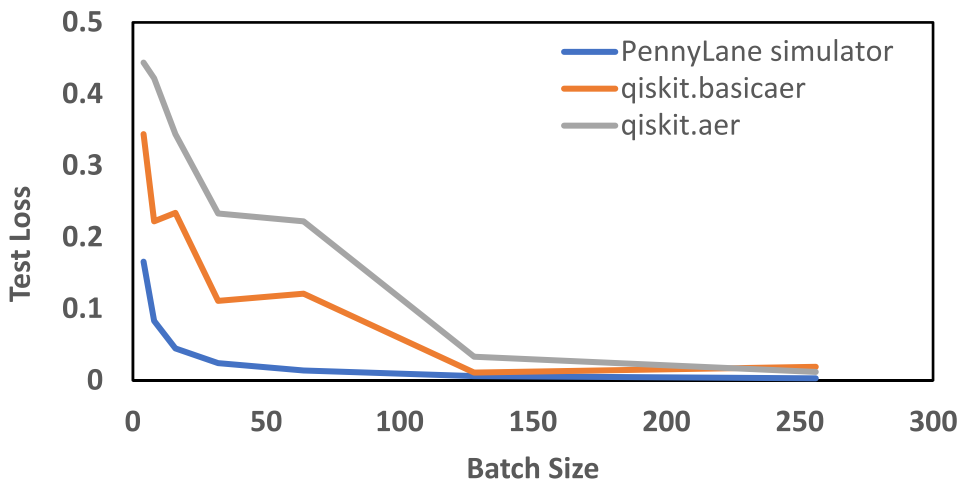


**Figure 12.** Test loss with respect to batch size for the classical–quantum neural network.

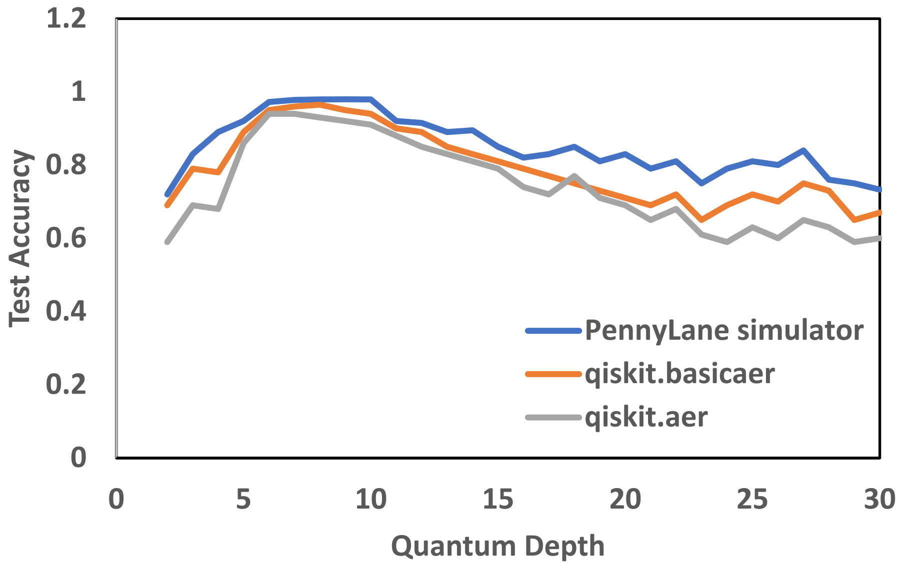


**Figure 13.** Test accuracy plot with respect to quantum depth for the classical–quantum neural network.

**Table 7.** Comparison of proposed quantum transfer learning method with existing state-of-the-art models.

| Author | Dataset | Model | Accuracy | Task |
|---|---|---|---|---|
| [36] | MRI | PBPSO features-based ResNet101 and DenseNet201 | 87.3% and 94.8% | Multi classification |
| [37] | MRI | DemNet | 95.23% | Multi classification |
| [38] | MRI | LSTM | 94% | Binary classification |
| [39] | MRI | DCNN<br>VGG-16<br>VGG-19 | 71%<br>77.04%<br>77.66% | Multi classification |
| [40] | MRI | 3D ResNet-18 | 88.5% | Binary classification |
| [41] | MRI | Inception<br>MobileNet<br>BellCNN | 86%<br>82%<br>95% | Binary classification |
| [42] | MRI | 3D CNN | 50.1% | Binary classification |
| [43] | MRI | 3D VGG-16 | 73.4% | Binary classification |
| [44] | MRI<br>PET | 3D CNN | 84.97%<br>88.08% | Binary classification |
| [45] | MRI | MobileNet | 85% | Binary classification |
| [46] | MRI | VGG-19 | 90.02% | Binary classification |
| **Proposed Method** | **MRI** | **Hybrid classical–quantum convolutional neural network based on ResNet34** | **97%** | **Binary classification** |

## 5. Conclusions

This work implemented a hybrid quantum–classical architecture for the automated detection of Alzheimer's disease. The classical learning network was modeled in GoogleNet/ResNet34 and confirmed against MRI images. The quantum transfer variational model established an improved and time-efficient classification of Alzheimer's disease that was further validated using various simulators, including the PennyLane, qiskit.aer and qiskit.basicaer quantum simulators.

Hybrid classical–quantum implementation using a dressed quantum circuit achieved dimensionality reduction via compact representation and detailed feature extraction, in contrast to classical deep learning networks. Therefore, in this work, we performed the experiments using a classical transfer learning algorithm and a quantum transfer learning algorithm, and then intercomparative performance analysis was performed to define the best algorithm for Alzheimer's detection. The experimental analysis showed that hybrid classical–quantum neural networks are able to add value to the healthcare industry. They are able to speed up complex computational algorithms, showing high accuracy while also increasing the performance of the model. Furthermore, the model can be optimized by hyper-tuning the batch size and the quantum depth of the variational circuit, making it a viable solution for real-time clinical settings.

**Author Contributions:** Conceptualization, T.S. and J.Z.; methodology, T.S., J.Z. and A.A.; software, T.S., J.Z. and H.Z.; validation, T.S., J.Z., A.U.R. and M.S.; formal analysis, T.S., M.S., A.A. and H.H.; investigation, J.Z., A.A., M.S., A.U.R. and H.H.; data curation T.S., J.Z. and H.H.; writing—original draft preparation, T.S., J.Z., A.U.R. and A.A.; writing—review and editing, T.S., J.Z., A.A., H.Z., A.U.R., M.S. and H.H.; supervision J.Z. and A.U.R.; project administration, H.Z., M.S. and H.H.; funding acquisition, A.A. and H.H. All authors have read and agreed to the published version of the manuscript.

**Funding:** This work was supported by King Saud University, Riyadh, Saudi Arabia, through Researchers Supporting Project number RSP-2021/184. The authors also thank Natural Sciences and Engineering Research Council of Canada (NSERC) and New Brunswick Innovation Foundation (NBIF) for the financial support of the global project. These granting agencies did not contribute in the design of the study and collection, analysis, and interpretation of data.

**Data Availability Statement:** Data are publicly available at https://www.kaggle.com/tourist55/alzheimers-dataset-4-class-of-images, accessed on 3 January 2022.

**Acknowledgments:** This work was supported by King Saud University, Riyadh, Saudi Arabia, through Researchers Supporting Project number RSP-2021/184. The authors also thank Natural Sciences and Engineering Research Council of Canada (NSERC) and New Brunswick Innovation Foundation (NBIF) for the financial support of the global project. These granting agencies did not contribute to the design of the study or the collection, analysis, and interpretation of data.

**Conflicts of Interest:** The authors declare no conflict of interest.

## References

1. Weidner, W.; Barbarino, S.P. The state of the art of dementia research: New frontiers. *Alzheimer's Dement. J. Alzheimer's Assoc.* **2019**, *6*, 4–443.
2. Islam, J.; Zhang, Y. Brain MRI analysis for Alzheimer's disease diagnosis using an ensemble system of deep convolutional neural networks. *Brain Inform.* **2018**, *5*, 2. [CrossRef] [PubMed]
3. Bibi, N.; Sikandar, M.; Din, I.; Almogren, A.; Ali, S. IoMT-based automated detection and classification of leukemia using deep learning. *J. Healthc. Eng.* **2020**, *2020*, 6648574. [CrossRef] [PubMed]
4. Almogren, A.; Mohiuddin, I.; Din, I.; Almajed, H.; Guizani, N. Ftm-iomt: Fuzzy-based trust management for preventing sybil attacks in internet of medical things. *IEEE Internet Things J.* **2020**, *8*, 4485–4497. [CrossRef]
5. Khan, S.R.; Sikandar, M.; Almogren, A.; Din, I.; Guerrieri, A.; Fortino, G. IoMT-based computational approach for detecting brain tumor. *Future Gener. Comput. Syst.* **2020**, *109*, 360–367. [CrossRef]
6. Almogren, A. An automated and intelligent Parkinson disease monitoring system using wearable computing and cloud technology. *Clust. Comput.* **2019**, *22*, 2309–2316. [CrossRef]
7. Basaia, S.; Agosta, F.L. Automated classification of Alzheimer's disease and mild cognitive impairment using a single MRI and deep neural networks. *NeuroImage Clin.* **2019**, *21*, 101645. [CrossRef]
8. Tufail, A.B.; Ma, Y.K.; Kaabar, M.K.; Rehman, A.U.; Khan, R.; Cheikhrouhou, O. Classification of initial stages of Alzheimer's disease through PET neuroimaging modality and deep learning: Quantifying the impact of image filtering approaches. *Mathematics* **2021**, *9*, 3101. [CrossRef]
9. Venugopalan, J.; Tong, L.; Hassanzadeh, H.R.; Wang, M.D. Multimodal deep learning models for early detection of Alzheimer's disease stage. *Sci. Rep.* **2021**, *11*, 3254. [CrossRef]
10. Pan, D.; Zeng, A.; Jia, L.; Huang, L.; Frizzell, T.; Song, X. Early Detection of Alzheimer's Disease Using Magnetic Resonance Imaging: A Novel Approach Combining Convolutional Neural Networks and Ensemble Learning. *Front. Neurosci.* **2020**, *14*, 259. [CrossRef]
11. Luo, S.; Li, X.; Li, J. Automatic Alzheimer's disease recognition from mri data using deep learning method. *J. Appl. Math. Phys.* **2017**, *5*, 1892–1898. [CrossRef]

12. Billones, C.D.; Demetria, O. DemNet: A Convolutional Neural Network for the detection of Alzheimer's Disease and Mild Cognitive Impairment. In Proceedings of the IEEE Region 10 Conference (TENCON), Singapore, 22–25 November 2016; IEEE: Piscataway, NJ, USA, 2017; Volume 11, pp. 3724–3727.
13. Sarraf, S.; Tofighi, G. Classifcation of alzheimer's disease using fmri data and deep learning cnns. *arXiv* **2016**, arXiv:1603.08631.
14. Kazemi, Y.; Houghten, S.K. A deep learning pipeline to classify different stages of Alzheimer's disease from fMRI data. In Proceedings of the IEEE Conference on Computational Intelligence in Bioinformatics and Computational Biology, St. Louis, MO, USA, 30 May–2 June 2018; Volume 11, p. 8404980.
15. Farhi, E.; Neven, H. Classification with quantum neural networks on near term processors. *arXiv* **2018**, arXiv:1802.06002.
16. Schuld, M.; Bocharov, A.; Krysta, M.S.; Wiebe, N. Circuit-centric quantum classifiers. *Phys. Rev. A* **2020**, *101*, 032308. [CrossRef]
17. Li, Y.; Zhou, R.G.; Xu, R. A quantum deep convolutional neural network for image recognition. *Quantum Sci. Technol.* **2020**, *5*, 044003. [CrossRef]
18. Li, J.; Alam, M.; Sha, C.M. Drug discovery approaches using quantum machine learning. *arXiv* **2021**, arXiv:2104.00746.
19. Solenov, D. The Potential of Quantum Computing and Machine Learning to Advance Clinical Research and Change the Practice of Medicine. *Mo. Med.* **2018**, *115*, 463–467.
20. Lu, Z.; Shen, P.; Deng, D. Markovian quantum neuroevolution for machine learning. *Phys. Rev. Appl.* **2021**, *16*, 044039. [CrossRef]
21. Mathur, N.; Landman, J. Medical image classification via quantum neural networks. *arXiv* **2021**, arXiv:2109.01831.
22. Jamal, A.T.; Ishak, A.B.; Khalek, S.A. Tumor edge detection in mammography images using quantum and machine learning approaches. *Neural Comput. Appl.* **2021**, *33*, 7773–7784. [CrossRef]
23. Duan, B. Quantum algorithm and quantum circuit for a-optimal projection: Dimensionality reduction. *Phys. Rev. A* **2019**, *99*, 032311. [CrossRef]
24. Mogalapalli, H. Classical–Quantum Transfer Learning for Image Classification. *SN Comput. Sci.* **2022**, *3*, 20. [CrossRef]
25. Alavi, A.; Akhoundi, H. Hybrid Classical-Quantum method for Diabetic Foot Ulcer Classification. *arXiv* **2021**, arXiv:2110.02222.
26. Zen, R.; Long, M.; Tan, R.; Hébert, F. Transfer learning for scalability of neural-network quantum states. *Phys. Rev. E* **2020**, *101*, 053301. [CrossRef]
27. Killoran, N.; Thomas, R.B.; Arrazola, J.M.; Schuld, M.; Quesad, N.; Lloyd, S. Continuous-variable quantum neural networks. *Phys. Rev. Res.* **2019**, *1*, 033063. [CrossRef]
28. Piat, S.; Usher, N.; Severini, S. Image classification with quantum pre-training and auto_encoders. *Int. J. Quantum Inf.* **2018**, *16*, 1840009. [CrossRef]
29. Sadiq, M.T.; Yu, X.; Yuan, Z.; Fan, Z.; Rehman, A.U.; Li, G.; Xiao, G. Motor Imagery EEG Signals Classification Based on Mode Amplitude and Frequency Components Using Empirical Wavelet Transform. *IEEE Access* **2019**, *7*, 127678–127692. [CrossRef]
30. Mari, A.; Thomas, R.B.; Izaac, J.; Schuld, M.; Killoran, N. Transfer learning in hybrid classical-quantum neural networks. *Quantum* **2020**, *4*, 340. [CrossRef]
31. Marella, S.T.; Parisa, H.S.K. Introduction to Quantum Computing. 2020. Available online: Intechopen.com (accessed on 25 November 2021).
32. Dubey, S. Alzheimer's Dataset. 2020. Available online: https://www.kaggle.com/tourist55/alzheimers-dataset-4-class-of-images (accessed on 3 January 2022).
33. Yessou, H.; Sumbul, G.; Demir, B. A comparative study of deep learning loss functions for multi-label remote sensing image classification. In Proceedings of the IEEE International Geoscience and Remote Sensing Symposium (IGARSS), Waikoloa, HI, USA, 26 September–2 October 2020; Volume 1109, pp. 1349–1352.
34. Noman, S.M.; Arshad, J.; Zeeshan, M.; Rehman, A.U.; Haider, A.; Khurram, S.; Cheikhrouhou, O.; Hamam, H.; Shafiq, M. An Empirical Study on Diabetes Depression over Distress Evaluation using Diagnosis Statistical Manual and Chi-Square Method. *Int. J. Environ. Res. Public Health* **2021**, *18*, 3755. [CrossRef]
35. Bergholm, V.; Izaac, J.; Schuld, M.; Gogolin, C. PennyLane: Automatic differentiation of hybrid quantum classical computations. *arXiv* **2018**, arXiv:1811.04968.
36. El-Aal, S.A.; Ghali, N.I. A proposed recognition system for Alzheimer's disease based on deep learning and optimization algorithms. *J. Southwest Jiaotong Univ.* **2021**, *56*, 5. [CrossRef]
37. Murugan, S.; Venkatesa, N.C.; Sumithra, M.G.; Gao, X.Z.; Elakkiya, B.; Akila, M.; Manoharan, S. DEMNET: A deep learning model for early diagnosis of alzheimer diseases and dementia from MRI images. *IEEE Access* **2021**, *9*, 90319–90329. [CrossRef]
38. Akbari, H.; Sadiq, M.T.; Rehman, A.U.; Ghazvini, M.; Naqvi, R.A.; Payan, M.; Bagheri, H.; Bagheri, H. Depression recognition based on the reconstruction of phase space of EEG signals and geometrical features. *Appl. Acoust.* **2021**, *179*, 108078. [CrossRef]
39. Ajagbe, S.A.; Amuda, A.K.; Oladipupo, M.A.; Afe, O. Multi-classification of Alzheimer disease on magnetic resonance images (MRI) using deep convolutional neural network (DCNN) approaches. *Int. J. Adv. Comput. Res.* **2021**, *11*, 51–60. [CrossRef]
40. Guan, Z.; Kumar, R.; Fung, Y.R.; Wu, Y.; Fiterau, M. A Comprehensive Study of Alzheimer's Disease Classification Using Convolutional Neural Networks. *arXiv* **2019**, arXiv:1904.07950.
41. Hussain, W.; Sadiq, M.T.; Siuly, S.; Rehman, A.U. Epileptic Seizure Detection Using 1 D-Convolutional Long Short-Term Memory Neural Networks. *Appl. Acoust.* **2021**, *177*, 107941. [CrossRef]
42. Rehman, A.U.; Naqvi, R.A.; Rehman, A.; Paul, A.; Sadiq, M.T.; Hussain, D. A Trustworthy SIoT Aware Mechanism as an Enabler for Citizen Services in Smart Cities. *Electronics* **2020**, *9*, 918. [CrossRef]

43. Yagis, E.; Citi, L.; Diciotti, S.; Marzi, C.; Atnafu, S.W. 3D Convolutional Neural Networks for Diagnosis of Alzheimer's Disease via structural MRI. In Proceedings of the 2020 IEEE 33rd International Symposium on Computer-Based Medical Systems (CBMS), Rochester, MN, USA, 28–30 July 2020; pp. 65–70.
44. Liu, M.; Cheng, D.; Wang, K.; Wang, Y. Multi-Modality Cascaded Convolutional Neural Networks for Alzheimer's Disease Diagnosis. *Neuroinformatics* **2018**, *16*, 295–308. [CrossRef] [PubMed]
45. Oommen, L.; Chandran, S.; Prathapan, V.L. Early detection of Alzheimer's disease using deep learning techniques. *Int. Res. J. Eng. Technol.* **2020**, *7*. [CrossRef]
46. Raees, M.; Thomas, V. Automated detection of Alzheimer's Disease using Deep Learning in MRI. *J. Phys.* **2021**, *1921*, 012024.